

Supporting Information

CsPbBr₃ perovskite quantum dots grown within Fe-doped zeolite X with improved stability for sensitive NH₃ detections

Wan Wu, Chunyu Zhao, Mingyou Hu, Aizhao Pan,* Wei Xiong, and Yinghao Chen

Department of Chemistry, School of Chemistry, Xi'an Jiaotong University, Xianning West Road, 28, Xi'an 710049, China.

Corresponding Author

*Email: panaizhao2017032@xjtu.edu.cn

Experimental Sections

Materials

Sodium hydroxide (NaOH, Sinopharm Chemical Reagent Co., Ltd., AR), sodium silicate ($\text{Na}_2\text{SiO}_3 \cdot 9\text{H}_2\text{O}$, Sinopharm Chemical Reagent Co., Ltd., $w(\text{Na}_2\text{O}) = 19.3\% \sim 22.8\%$), sodium aluminate (NaAlO_2 , Sinopharm Chemical Reagent Co., Ltd., $w(\text{Al}_2\text{O}_3) \geq 41.1\%$), ferric nitrate ($\text{Fe}(\text{NO}_3)_3 \cdot 9\text{H}_2\text{O}$, Sinopharm Chemical Reagent Co., Ltd., AR), cesium bromide (CsBr, Macklin, 99.5%), oleic acid (OA, Bide Pharmatech Ltd., 90%), 1-octadecene (ODE, Meryer, 90%), oleylamine (OLAm, Aladdin, $w(\text{C18}) = 80\% \sim 90\%$), lead bromide (PbBr_2 , Shanghai Yuanye Biotechnology Co., Ltd., AR), n-hexane (C_6H_{14} , Sinopharm Chemical Reagent Co., Ltd., AR), isopropanol (IPA, Fuyu Chemicals, AR), ammonia solution (Fuyu Chemicals, AR), and calcium oxide (CaO , Sinopharm Chemical Reagent Co., Ltd., AR) were straightway used without purifications.

Characterization

Powder X-ray diffraction (PXRD) patterns were acquired using a Bruker AXS D8 Discover X-Ray Diffractometer with a wavelength of 1.79 \AA (Cu $K\alpha$ radiation). X-ray photoelectron spectroscopy (XPS) measurements were conducted on an AXIS ULTRA (England, KRATOS ANALYTICAL Ltd.) using an Al mono $K\alpha$ X-ray source (1486.6 eV) at 150 W. Scanning electron microscopy (SEM) images were gained on a JEOL 7800F Field-Emission Scanning Electron Microscope. Transmission electron microscopy (TEM), high-resolution TEM (HR-TEM) and energy dispersive X-ray spectrum (EDX) elemental mapping results were achieved on a FEI G2F30 electron microscope operated at 200 kV with a Gatan SC 200 CCD camera. Inductively coupled plasma (ICP) analysis was measured with a Perkin-Elmer Optima 3300 DV ICP instrument. The steady-state photoluminescence spectra (PL) were collected using a F-4600 Fluorescence spectrophotometer (Hitachi) under excitation at 365 nm. The time-resolved fluorescence measurements were detected with a FLS-1000 steady state and transient state fluorescence spectrometer (Edinburgh Instruments Ltd.). Acidic properties were investigated adopting temperature-programmed desorption of ammonia

(NH₃-TPD) using an Auto Chem II 2920 analyser. The Brunauer-Emmet-Teller (BET) and Barrett-Joyner-Halenda (BJH) methods were characterized for pore size distributions and specific surface areas by an ASAP 2020 Micrometrics sorptometer (USA).

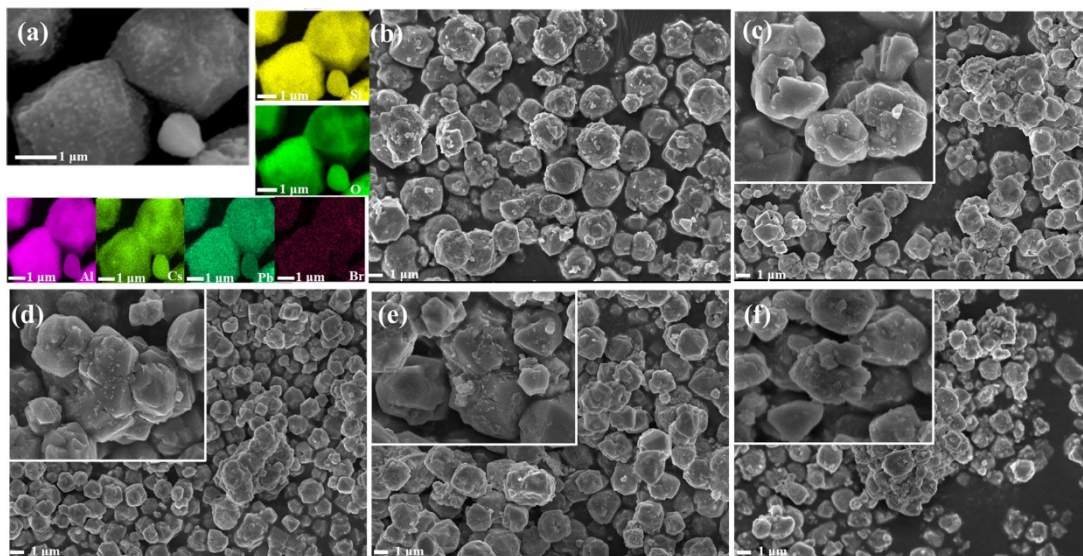


Figure S1. TEM elemental mapping profiles for Si, O, Al, Cs, Pb and Br of QDs/X (a), SEM images of QDs/X (b),

QDs@Fe/X-1 (c), QDs@Fe/X-2 (d), QDs@Fe/X-3 (e), and QDs@Fe/X-4 (f)

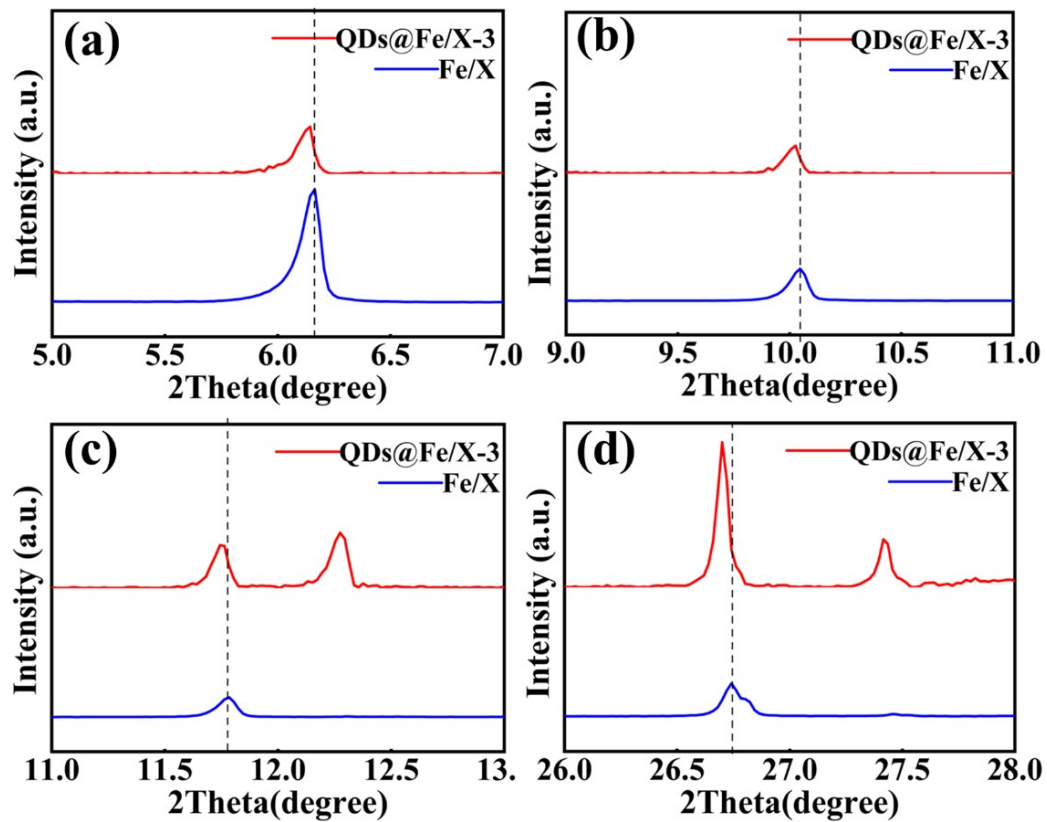


Figure S2. Locally-amplified XRD patterns: $2\theta = 5^\circ\sim 7^\circ$ (a); $2\theta = 9^\circ\sim 11^\circ$ (b); $2\theta = 11^\circ\sim 13^\circ$ (c); $2\theta = 26^\circ\sim 28^\circ$ (d)

Table S1. PL decay parameters of the QDs/X and QDs@Fe/X-n

Samples	τ_1/ns	$A_1/\%$	τ_2/ns	$A_2/\%$	$\tau_{\text{average}}/\text{ns}$
QDs/X	5.22	34.95	36.15	65.06	25.35
QDs@Fe/X-1	5.90	26.53	36.05	73.47	28.05
QDs@Fe/X-2	5.73	22.61	39.99	77.39	32.24
QDs@Fe/X-3	5.93	18.66	45.84	81.34	38.39
QDs@Fe/X-4	6.04	32.47	40.39	67.53	29.24

The decay data were fitted using a two-exponential decay model with low uncertainties (χ):

$$I(t) = A_1 e^{-t/\tau_1} + A_2 e^{-t/\tau_2}$$

$$\tau_{\text{ave}} = \sum A_i \tau_i^2 / \sum A_i \tau_i$$

wherein, $I(t)$ refer to the time-dependent fluorescence intensity, and A , τ and τ_{ave} mean the amplitude, lifetime and average lifetime respectively.

Table S2 Composition and textural properties of Fe/X and QDs@Fe/X-3

Sample	$S_{\text{BET}}(\text{m}^2/\text{g})$	$V_{\text{micro}}(\text{cm}^3/\text{g})$
Fe/X	891.0	0.299
QDs@Fe/X-3	166.1	0.051

Table S3. Summary of the comparison of perovskite-based sensors and QDs-based optical sensors for ammonia reported in the literature.

Samples	Testing gas	Stability	Response	Ref.
		Time	($R = R_g/R_a$)	
CsPbBr ₃ /BNNF	NH ₃	96 h	96%	1
CsPbBr ₃ QDs	NH ₃	125 h	80%	2
Cu ₁₂ Sb ₄ S ₁₃ QDs/rGO	NH ₃	30 d	97.3%	3
PbS QDs/rGO	NH ₃	31 d	94%	4
BP-SnO-4	NH ₃	28 d	60%	5
TiO ₂ QDs	NH ₃	45 d	100%	6
SnO ₂ QDs@MoS ₂	NH ₃	30 d	75%	7
QDs@Fe/X-3	NH ₃	100 d	98%	In this work

Notes and references

- 1 X. He, C. Yu, M. Yu, J. Lin, Q. Li, Y. Fang, Z. Liu, Y. Xue, Y. Huang and C. Tang, *Inorganic Chemistry*, 2020, **59**, 1234–1241
- 2 H. Huang, M. Hao, Y. Song, S. Dang, X. Liu and Q. Dong, *Small*, 2020, **16**, 1904462.
- 3 Y. Liu, B. Sang, H. Wang, Z. Wu, Y. Wang, Z. Wang, Z. Peng and W. Chen, *Chinese Chemical Letters*, 2020, **31**, 2109-2114.
- 4 Y. Liu, H. Wang, S. Yang, K. Chen, T. Yang, J. Wei, J. Tian and W. Chen, *Sensors and Actuators B: Chemical*, 2018, **255**, 2979-2987.
- 5 H. Ren, Y. Zhou, Y. Wang, Y. Ou, C. Gao and Y. Guo, *Sensors and Actuators B: Chemical*, 2022, **365**, 131910.
- 6 H. Liu, W. Shen, X. Chen and J.-P. Corriou, *Journal of Materials Science: Materials in Electronics*, 2018, **29**, 18380-18387.
- 7 J. Bai, Y. Shen, S. Zhao, Y. Chen, G. Li, C. Han, D. Wei, Z. Yuan and F. Meng, *Sensors and Actuators B: Chemical*, 2022, **353**, 131191.